Non-relativistic Disk-wind-Driven Expanding Radio-emitting Shell in Tidal Disruption Events

Hayasaki & Yamazaki (2023), ApJ, 954, 5

Kimi Hayasaki
Chungbuk National University (SK)

「高エネルギー現象で探る宇宙の多様性IV」研究会@ICRR on 12/Nov/2024

Scientific motivation to study tidal disruption events (TDEs)

1. Probe of quiescent supermassive black holes (SMBHs) and intermediate-mass black holes
2. Natural laboratory for testing general relativistic (GR) effects
3. Luminous thermal transients over a wide range of wavebands from optical to UV to soft X-ray + IR from dust echoes
4. Sources for non-thermal, high-energy (e.g., synchrotron) emissions
5. Targets for multi-messenger astronomy: gravitational wave and neutrino sources (IceCube neutrino associated with AT2019dsg)

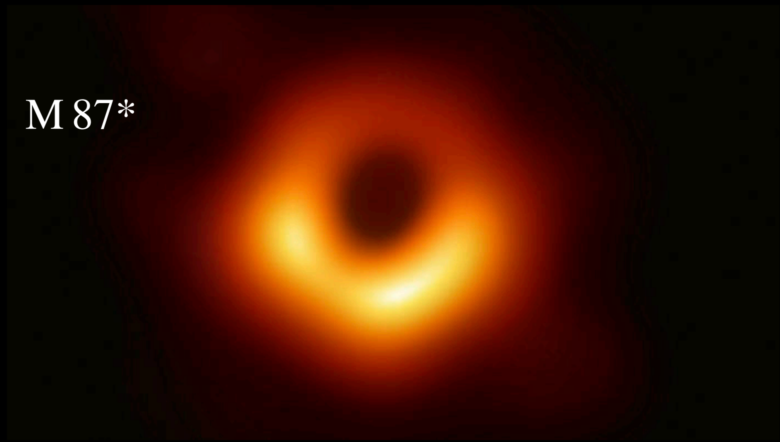

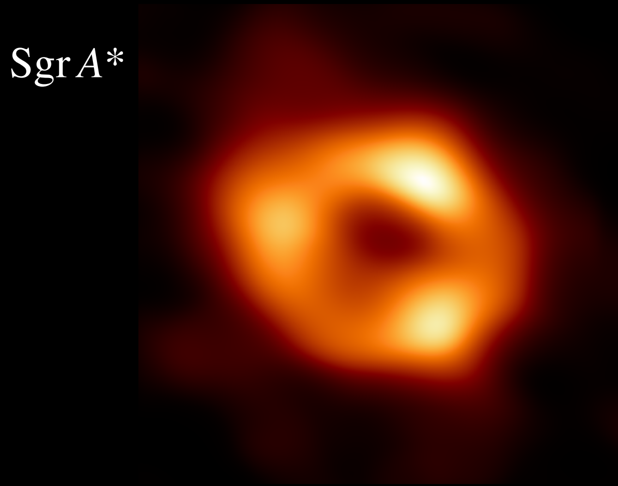

https://eventhorizontelescope.org/

EHT collaboration (2019) and (2022)

Condition for causing TDEs

$$r_\mathrm{t} \geq \zeta(a^*)\, r_\mathrm{S}$$

($\mathcal{O}(0.1) \leq \zeta \leq \mathcal{O}(1)$;
e.g., see Mummery 2024)

Hill's mass (Stone et al 2019; Rossi et al. 2020)

$$M \leq 10^8 M_\odot\, (\zeta/1.0)^{-3/2}\, (r_*/R_\odot)^{3/2} (m_*/M_\odot)^{-1/2}$$

Main sequence stellar disruptions likely happen at quiescent SMBHs with $M \leq 10^8 M_\odot$

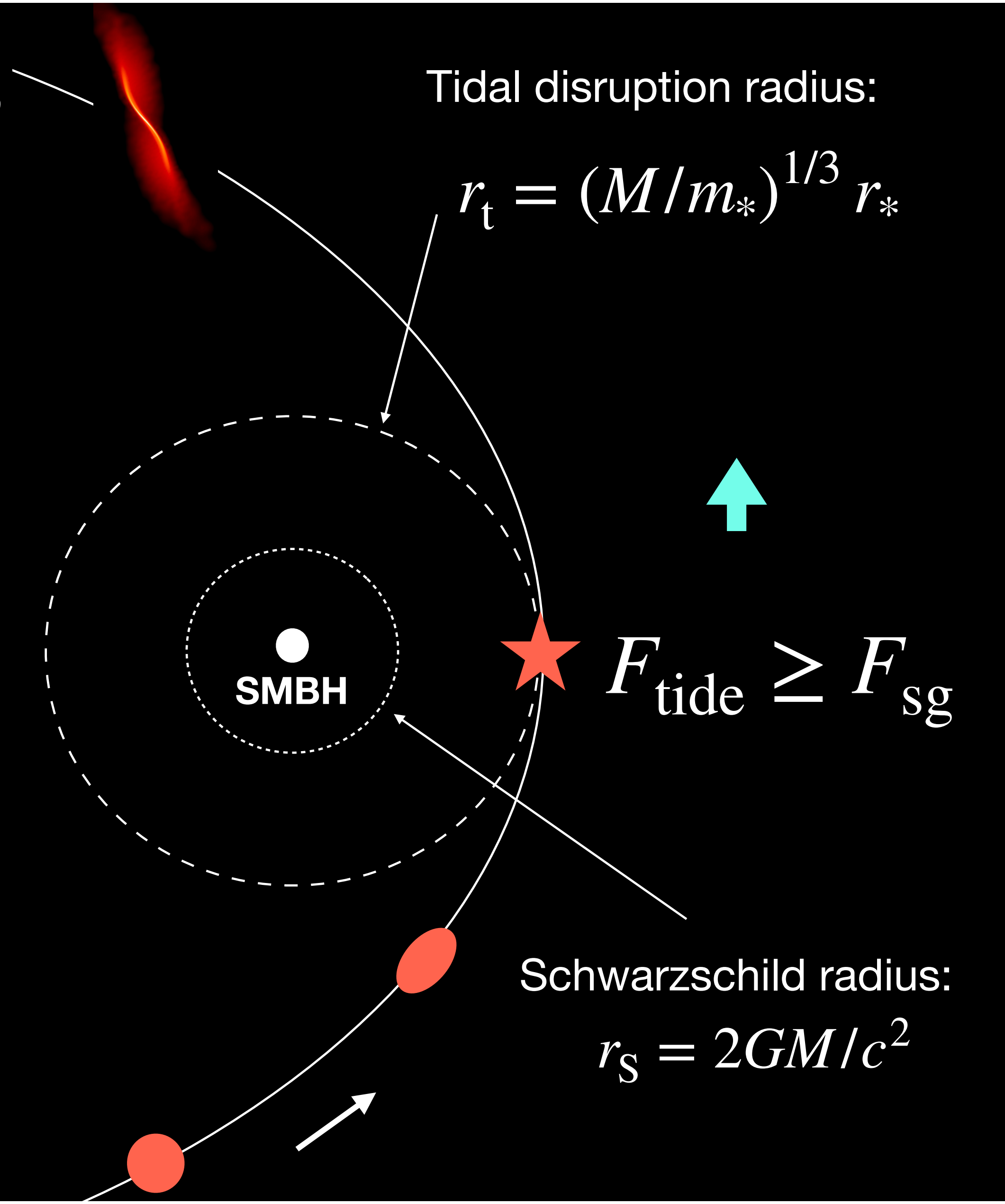

Overview of TDE theory

Standard picture of a TDE

Rees (1988)

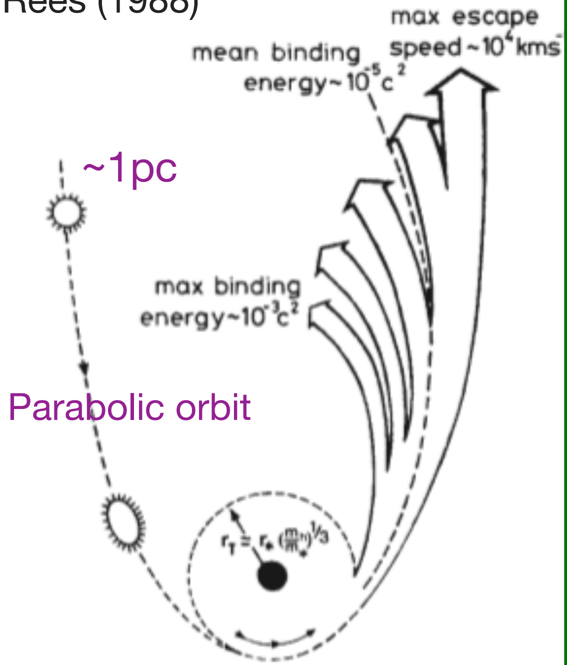

$$r_t \sim 5\, r_S\, M_7^{-2/3}\, m_{*,1}^{-1/3} r_{*,1}$$

Specific binding energy

$$\epsilon = 0 \rightarrow \epsilon = \pm \Delta\epsilon$$

Star — Stellar debris

$0 < \epsilon \leq \Delta\epsilon \rightarrow$ Unbound debris

$-\Delta\epsilon \leq \epsilon < 0 \rightarrow$ Bound debris

$$M_7 = M/10^7 M_\odot$$
$$m_{*,1} = m_*/M_\odot$$
$$r_{*,1} = r_*/R_\odot$$

- Debris spread energy

$$\Delta\epsilon/c^2 \approx (GM/r_t)(r_*/r_t)/c^2 \sim 4.6 \times 10^{-4}\ M_7^{1/3}\, m_{*,1}^{2/3}\, r_{*,1}^{-1}$$

- Fallback time of most tightly bound debris

$$t_{\rm mtb} = (\pi/\sqrt{2})(1/\Omega_*)\left(M_{\rm bh}/m_*\right)^{1/2} \sim 0.35\ {\rm yr}\ M_7^{1/2}\, m_*^{-1}\, r_*^{2/3}$$

- Peak mass fallback rate (super-Eddington rate)

$$\dot{M}_{\rm fb,pk} = (1/3)(m_*/t_{\rm mtb}) \sim 6 \times 10^{25}\, {\rm g\, s^{-1}}\, M_7^{-1/2}\, m_{*,1}^2\, r_{*,1}^{-3/2} \gg L_{\rm Edd}/c^2$$

($L_{\rm Edd} = 1.3 \times 10^{45}\, M_7\, {\rm erg/s}$ is the Eddington luminosity)

- Time dependence of mass fallback rate

$$\dot{M}_{\rm fb} = (d\mathscr{M}/d\epsilon)(d\epsilon/dt) \propto t^{-n}$$

$$n = \begin{cases} 5/3 & \text{w/o stellar internal structure} \\ < 5/3 & \text{w/ stellar internal structure} \\ > 5/3 & \text{partial TDEs} \\ > 5/3 & \text{eccetric TDEs} \\ < 5/3 & \text{hyperbolic TDEs} \end{cases}$$

- 5/3, w/o stellar internal structure: Rees (1988); Phinny(1989); Evans & Kochaneck (1989)
- < 5/3, w/ stellar internal structure: Lodato et al. (2009); Golightly et al. (2019)
- > 5/3, partial TDEs: Guillochon & Ramirez-Ruiz (2013); Coughlin & Nixon (2019)
- > 5/3, eccetric TDEs: Hayasaki et al. (2013, 2018); Park & Hayasaki (2021); Cufari et al. (2022)
- < 5/3, hyperbolic TDEs: Hayasaki et al. (2018); Park & Hayasaki (2021); Cufari et al. (2022)

Debris circularization and mass accretion rate

1. Circularization radius ($r_{\rm circ}$)

$$r_{\rm circ} = l^2/GM = \begin{cases} (1+e^*)r_{\rm t}/\beta & \text{for eccentric TDEs (Hayasaki et al. 2013)} \\ 2r_{\rm t} \sim 10\, r_{\rm S}\, (\beta/1.0)^{-1} M_7^{-2/3}\, m_{*,1}^{-1/3}\, r_{*,1} & \text{for standard, parabolic TDEs} \end{cases}$$

2. Circularization time ($t_{\rm circ}$)

Ballistic approximation for parabolic TDEs (Bonnerot et al. 2017)

$$t_{\rm circ} = 8.3\, \beta^{-3} (M/10^6 M_\odot)^{-5/3}\, t_{\rm mtb}$$
$$\sim 6.3 \times 10^{-2}\, {\rm yr}\, \left(\beta/1.0\right)^{-3} M_7^{-7/6}\, m_{*,1}^{-1}\, r_{*,1}^{3/2}$$

3. Mass accretion rate ($\dot{M}_{\rm acc}$)

$$t_{\rm acc} \le t_{\rm circ} \rightarrow \dot{M}_{\rm acc} = \dot{M}_{\rm fb}$$
$$t_{\rm acc} > t_{\rm circ} \rightarrow \dot{M}_{\rm acc} \neq \dot{M}_{\rm fb}$$

(Cannizzo et al. 1990, 2009;
Balbus 2017; Mummery & Balbus 2020;
Tamilan, Hayasaki & Suzuki 2024)

Accretion disk formation for the radiatively efficient case

Hayasaki, Stone & Loeb (2013)

Newtonian potential simulation

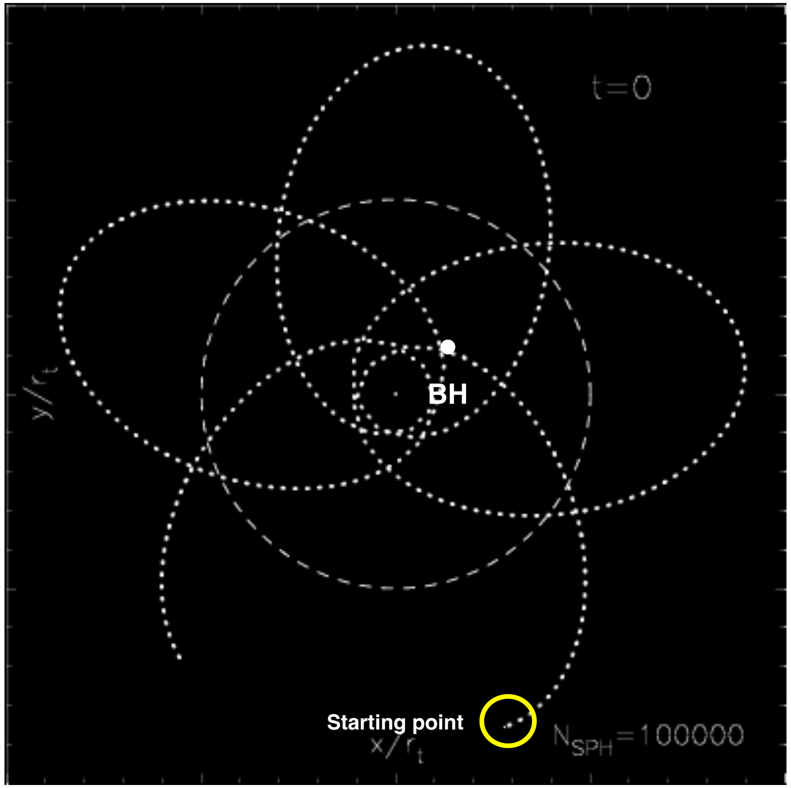

Simulation with GR corrections

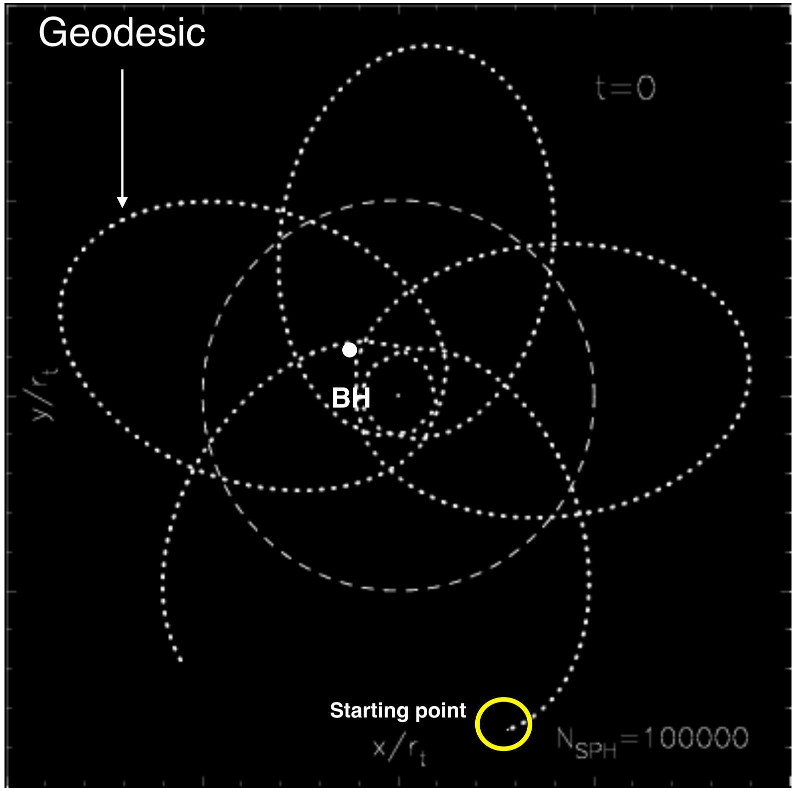

General relativistic precession plays a crucial role in the accretion disk formation around supermassive black hole

Optically thick case

- Potentially liberated energy due to stream-stream collision:

$$E_{\rm mtb} = GMm_*/4a_{\rm mtb} \sim 4.1 \times 10^{50}\,{\rm erg}\,M_7^{1/3}\,m_{*,1}^{5/3}\,r_{*,1}^{-1}$$

$$(a_{\rm mtb} \sim 10^{15}{\rm cm}\;M_7^{2/3} m_{*,1}^{-2/3}\,r_{*,1} \sim 107\,r_{\rm t})$$

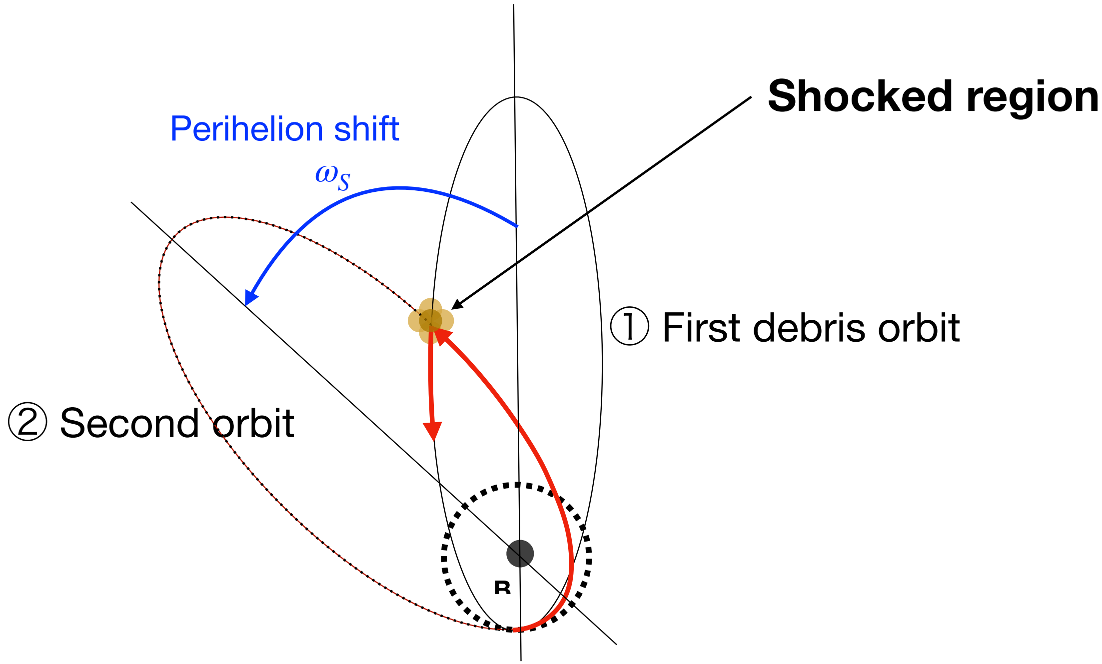

Edge-on view

Lu and Bonnerot (2020); Bonnerot and Lu (2020)

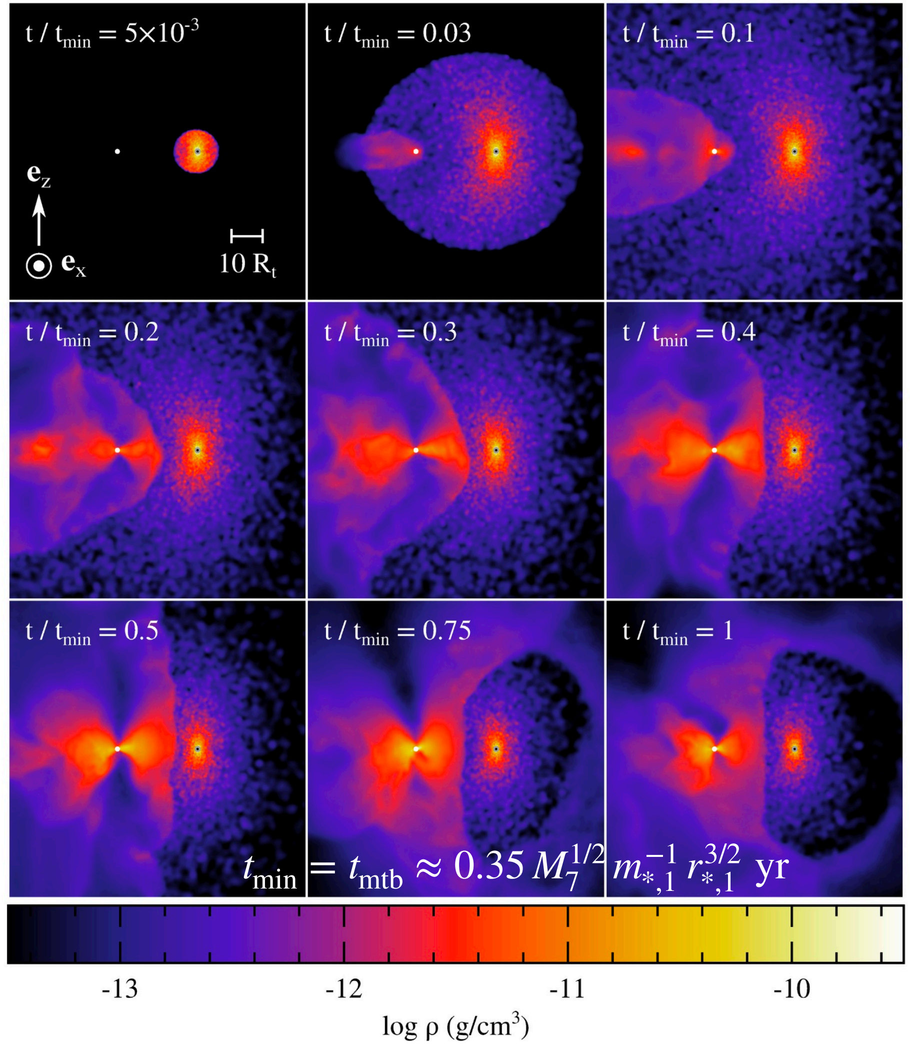

The two-stage simulation demonstrated that the outflow drives the disk formation.

Eddington envelope formation

Loeb & Ulmer (1997)

Self-consistent parabolic
TDE simulations by Price et al. (2024)

1. Outflow velocities of $\sim 10^4\,\mathrm{km/s}$;

2. Peak optical luminosities of $\lesssim L_{\mathrm{Edd}}$ at the large photosphere radii of $\sim 10 - 100\,\mathrm{AU}$;

3. A relatively low mass accretion rate ($\sim 10^2\,M_{\odot}/\mathrm{yr}$) due to the mass loss

4. Soft-X-ray emission from the formed disk could appear at late time due to collapse of the photosphere near BH.

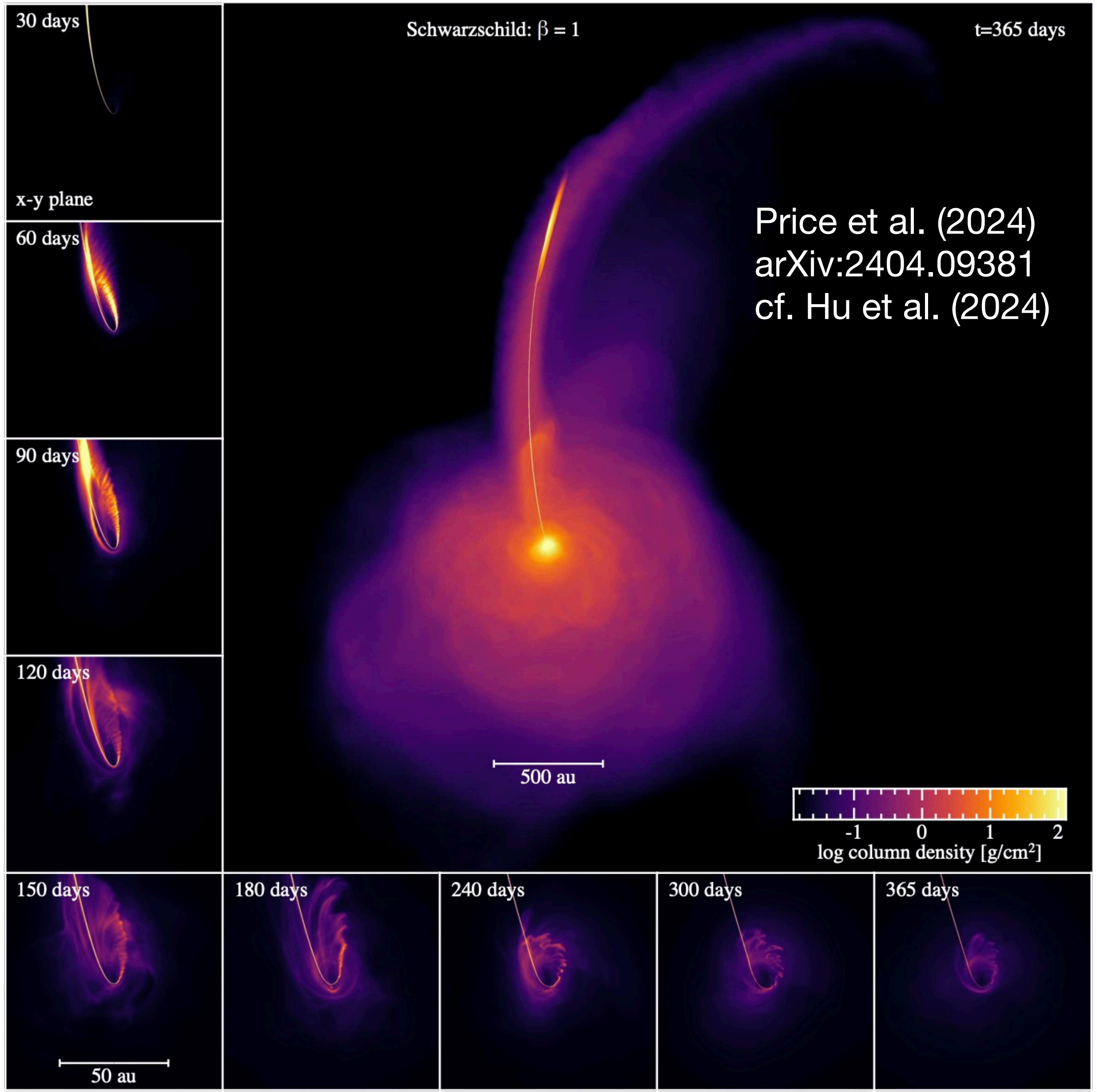

Price et al. (2024)
arXiv:2404.09381
cf. Hu et al. (2024)

Eddington envelope formation at a large scale and low density region

$t \leq 365$ days

Disk formation at the smaller scale and (much) higher density region

$t \geq 366$ days

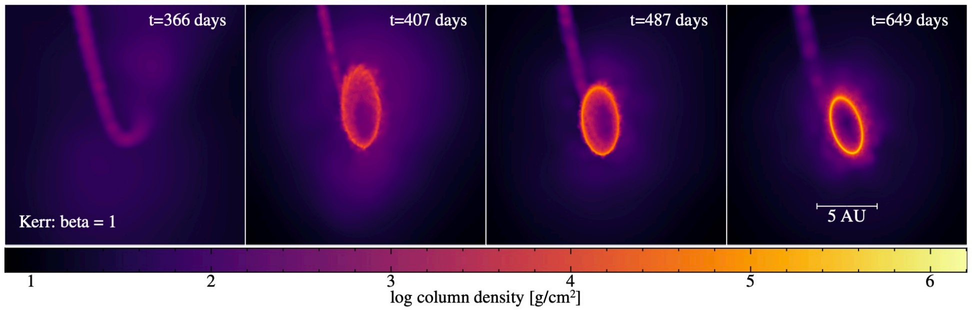

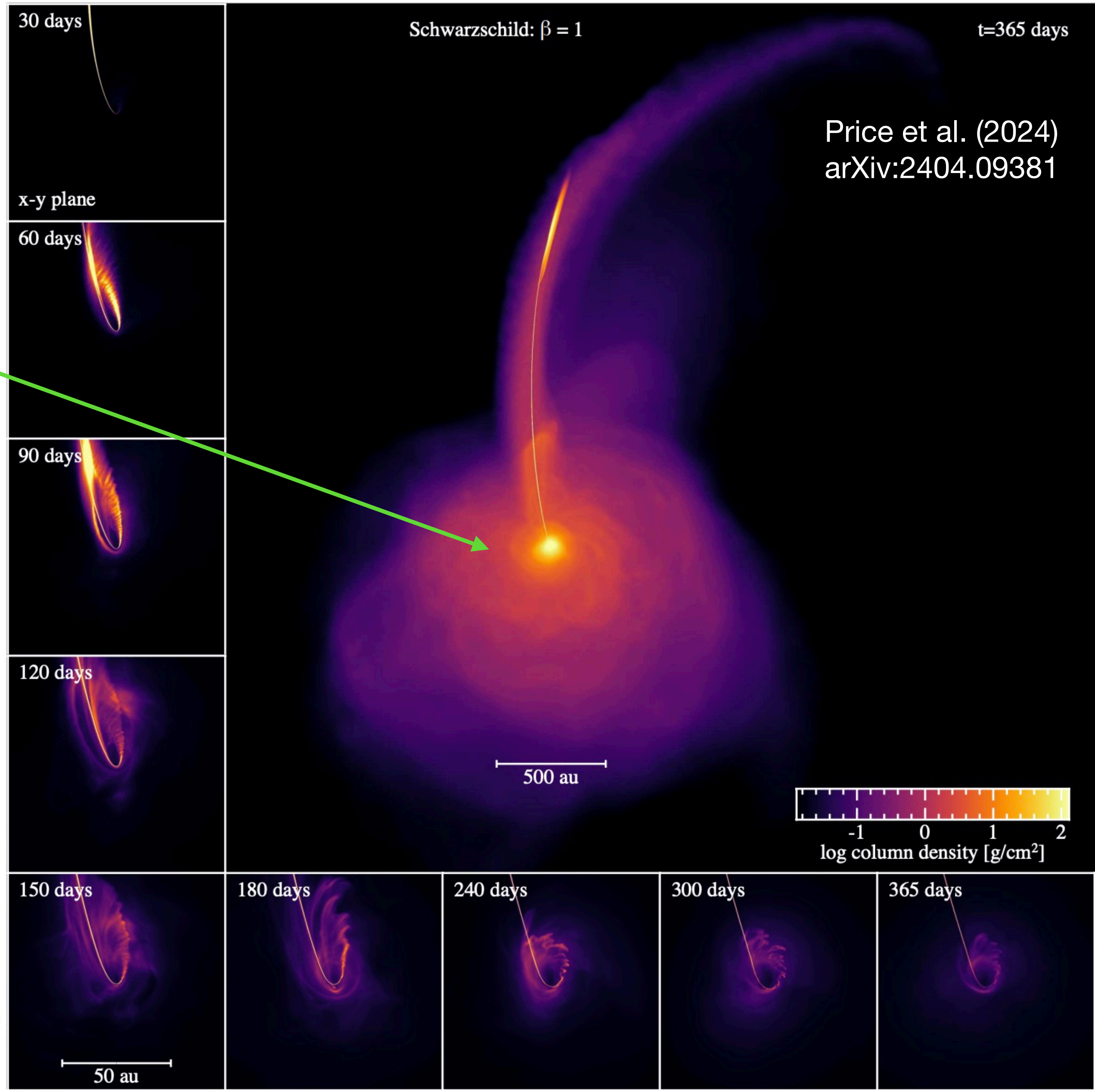

Importance of accretion disks in observed TDEs

1. Primary X-ray emission source, providing crucial insights into the energetics, dynamics, and emission mechanisms in X-ray-emitting TDEs.

2. Disk models can explain properties of TDE X-ray light curves

Suvi Gezari (2021)

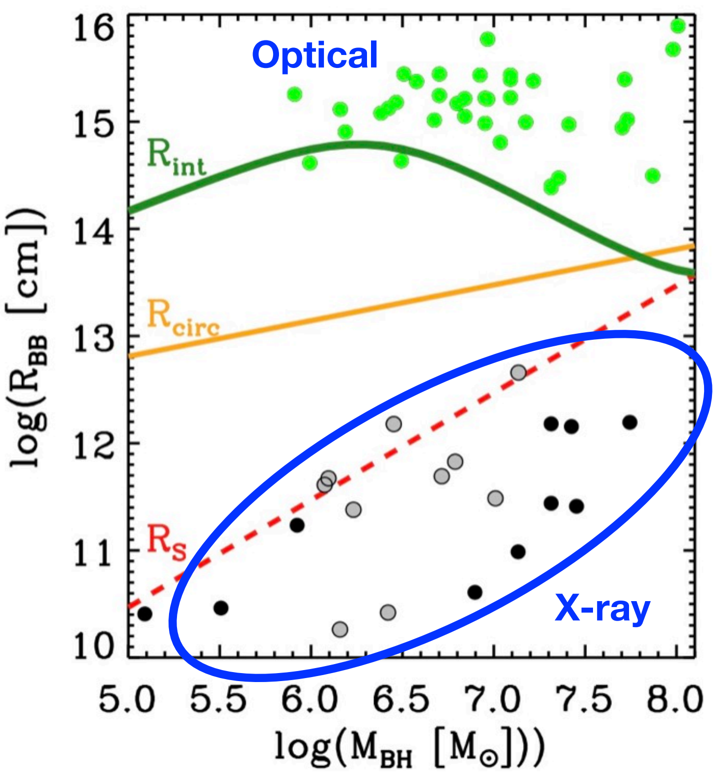

Power-law index (m): $L_X \propto \dot{M}_{acc} \propto t^{-m}$

Auchettl et al. (2017); Saxton et al.(2020)

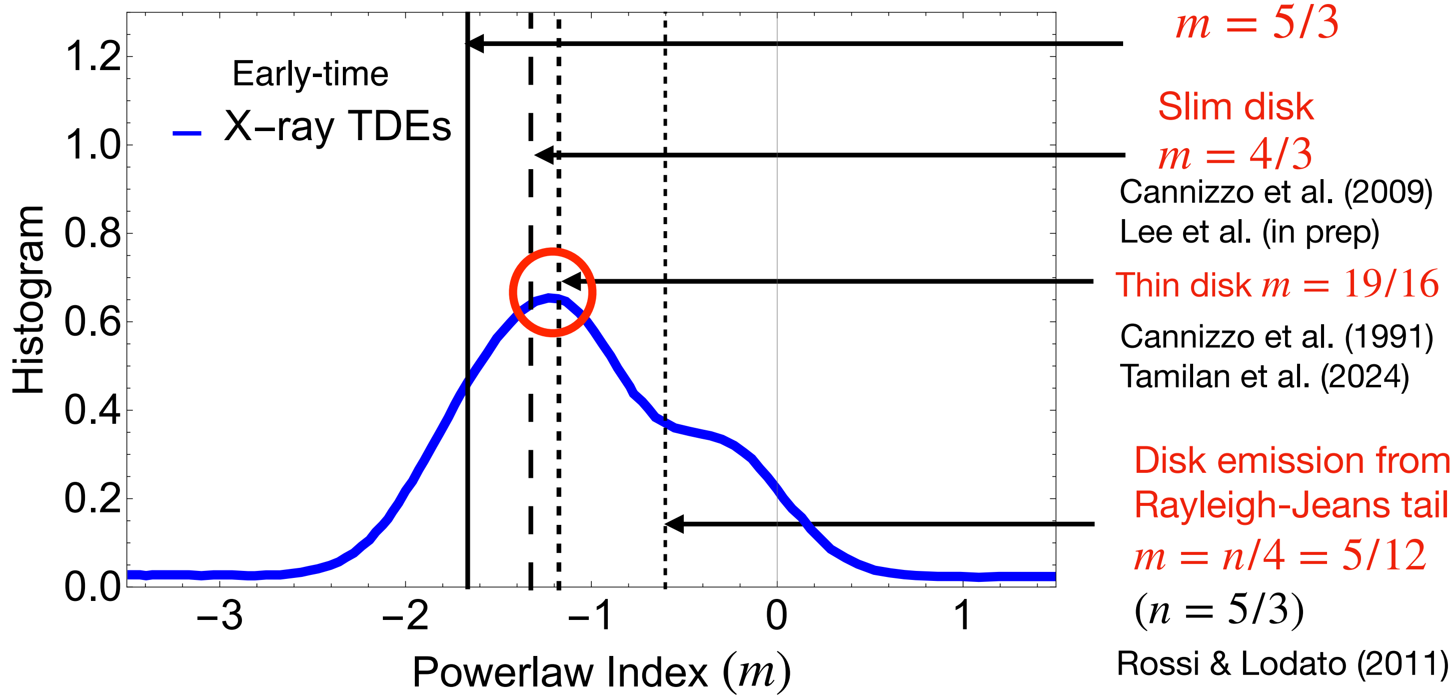

Radio observations of TDEs

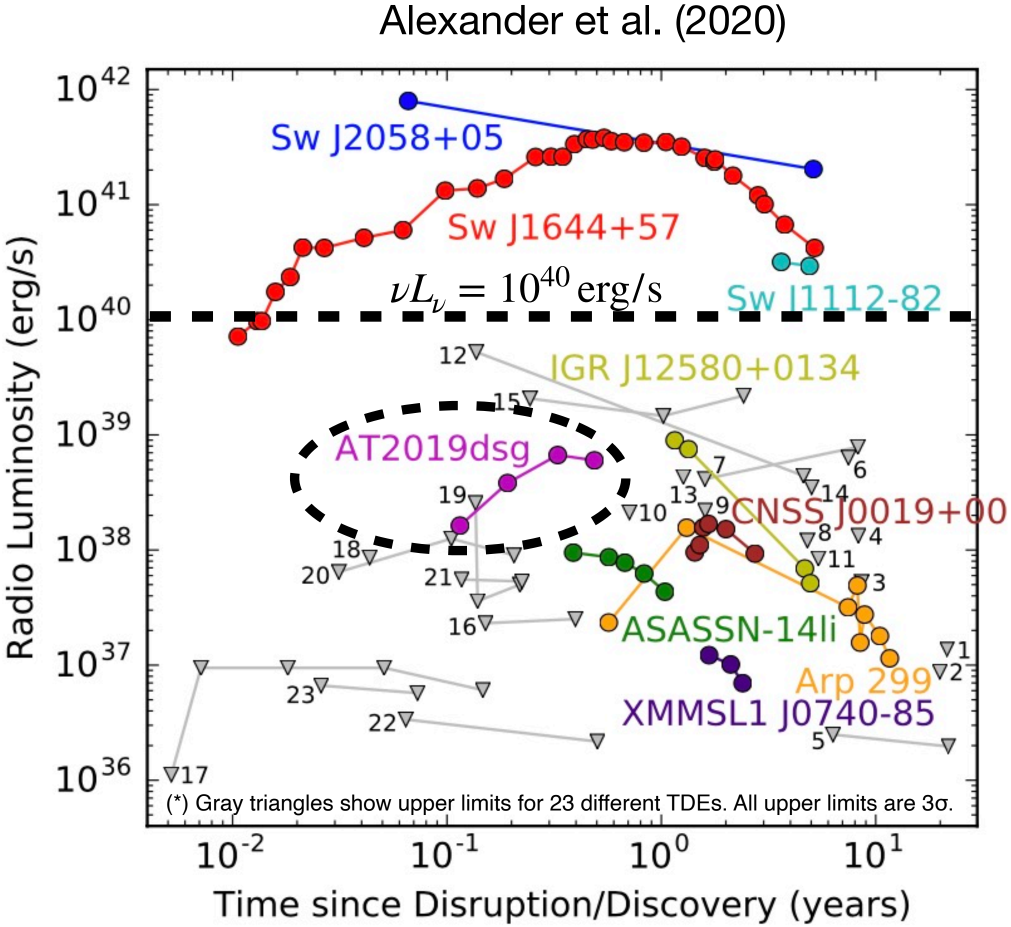

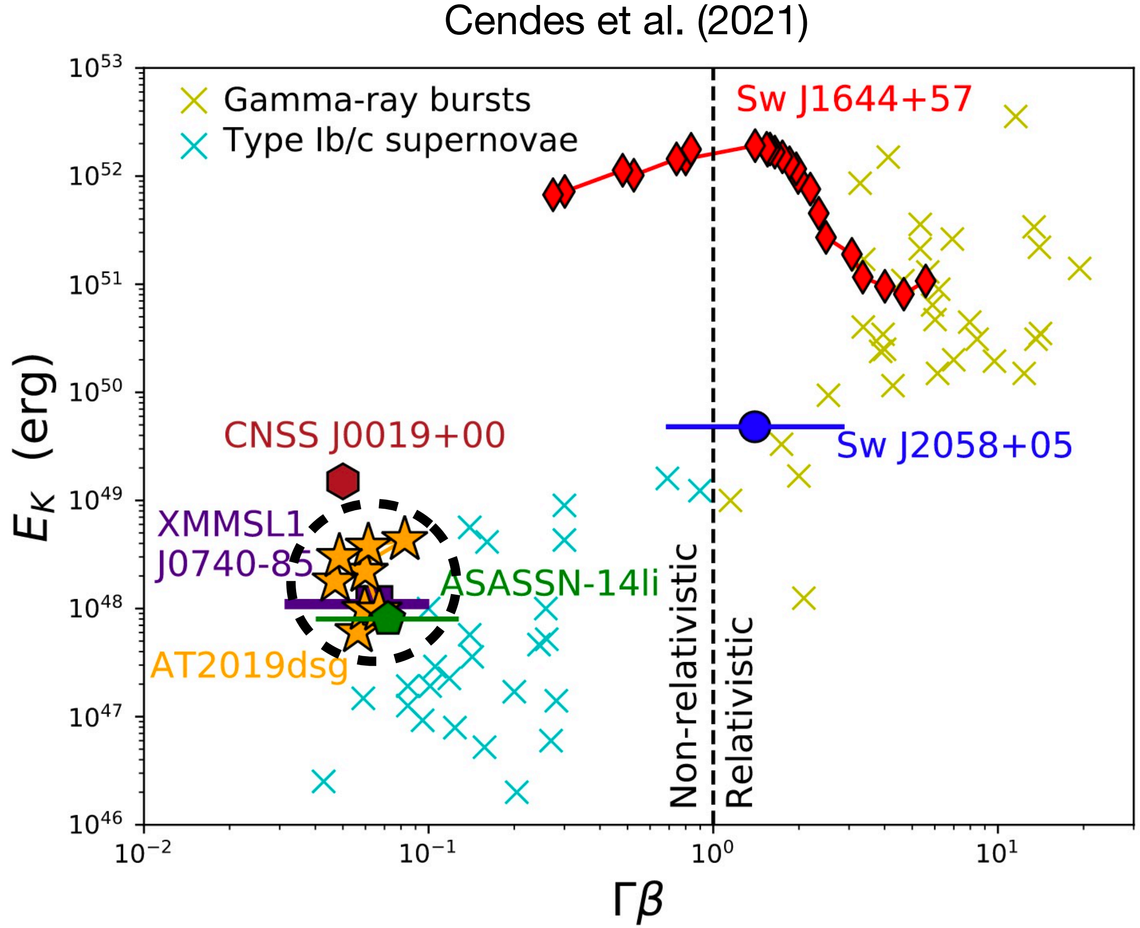

Outflow velocity is non-relativistic ($\beta \sim 0.1$) in AT2019dsg

Multi-wavelength observations of AT2019dsg

(Stein+2021; Cannizzaro+2021
van Velzen+2024)

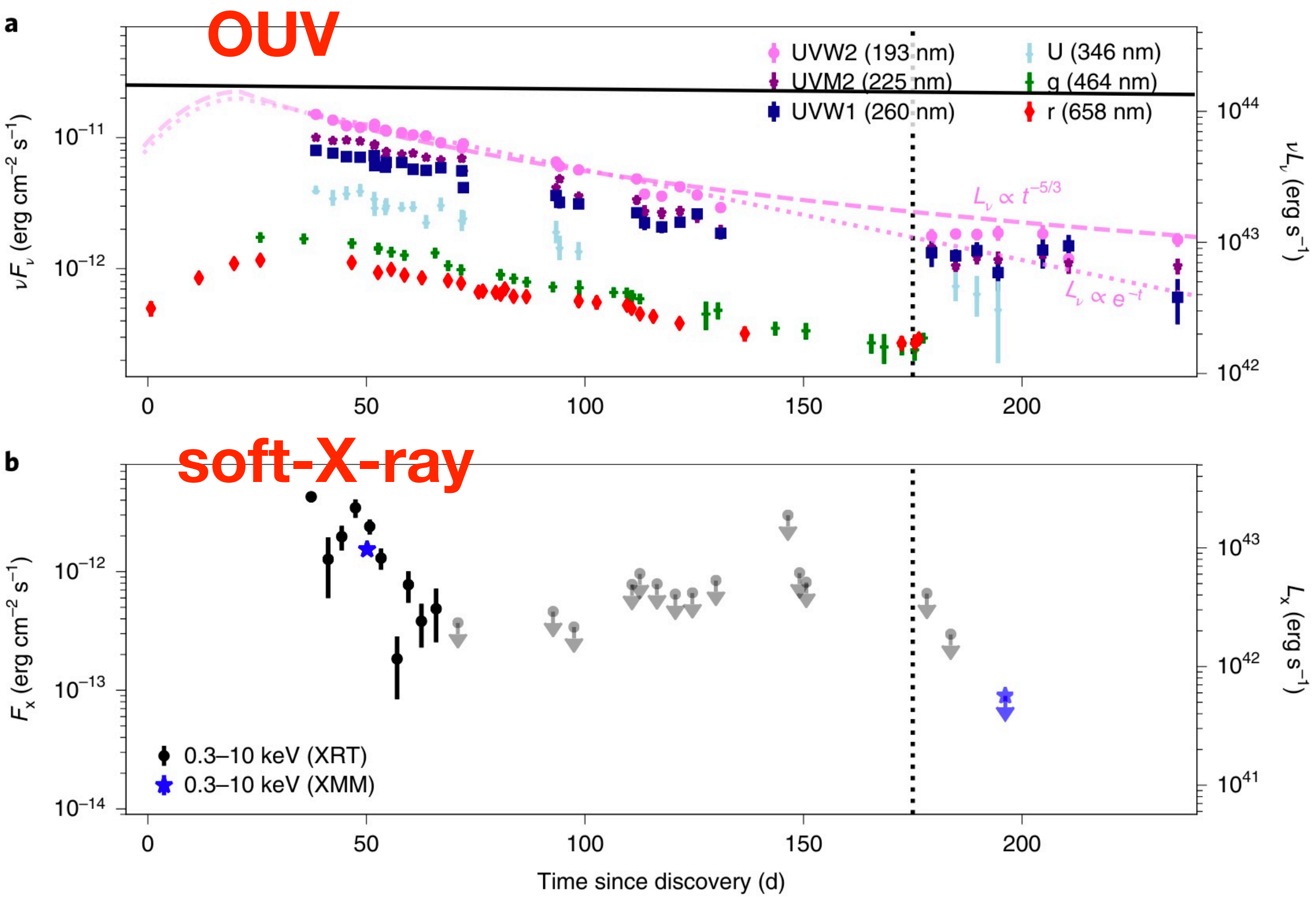

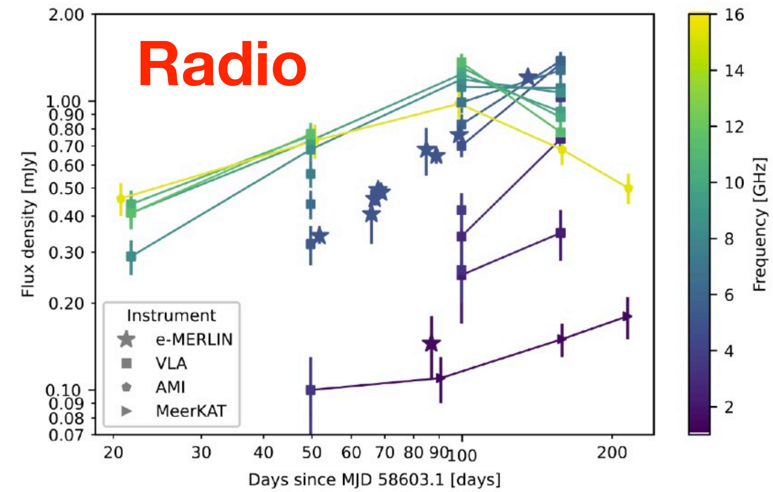

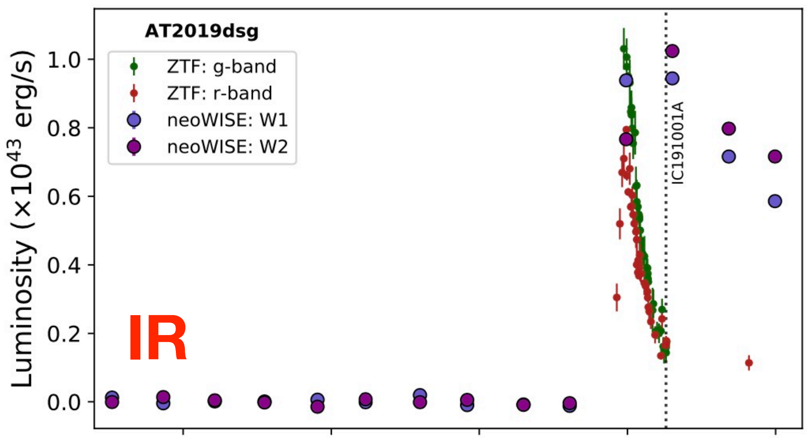

Flaring from **OUV** to **soft X-ray + radio** bands
with strong **IR** echo + **neutrino**

Strong dust echo

Evolution of radio emitted region in AT2019dsg

Equipartition analysis (with ν_p and F_p by fitting the observed data to theoretical SSA spectrum) gives $R(t)$

Stein et al. (2021)

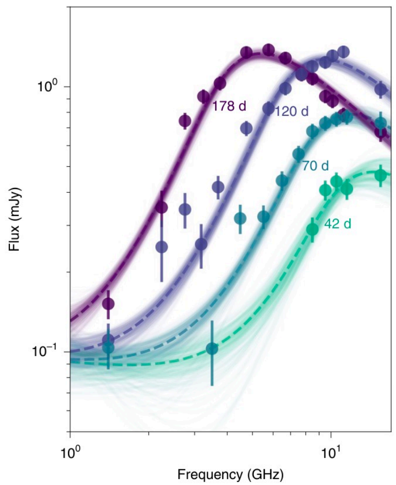

Granot & Sari (2002)

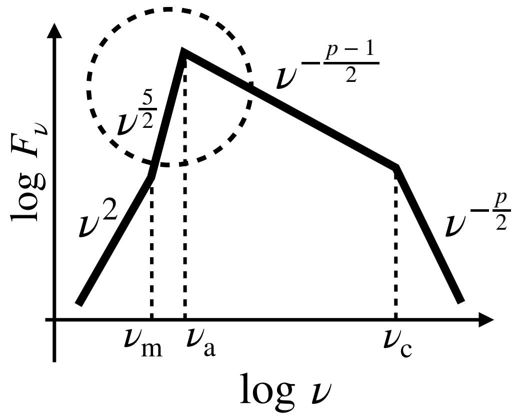

SSA spectrum with $\nu_\mathrm{m} < \nu_a$

Cendes et al. (2021)

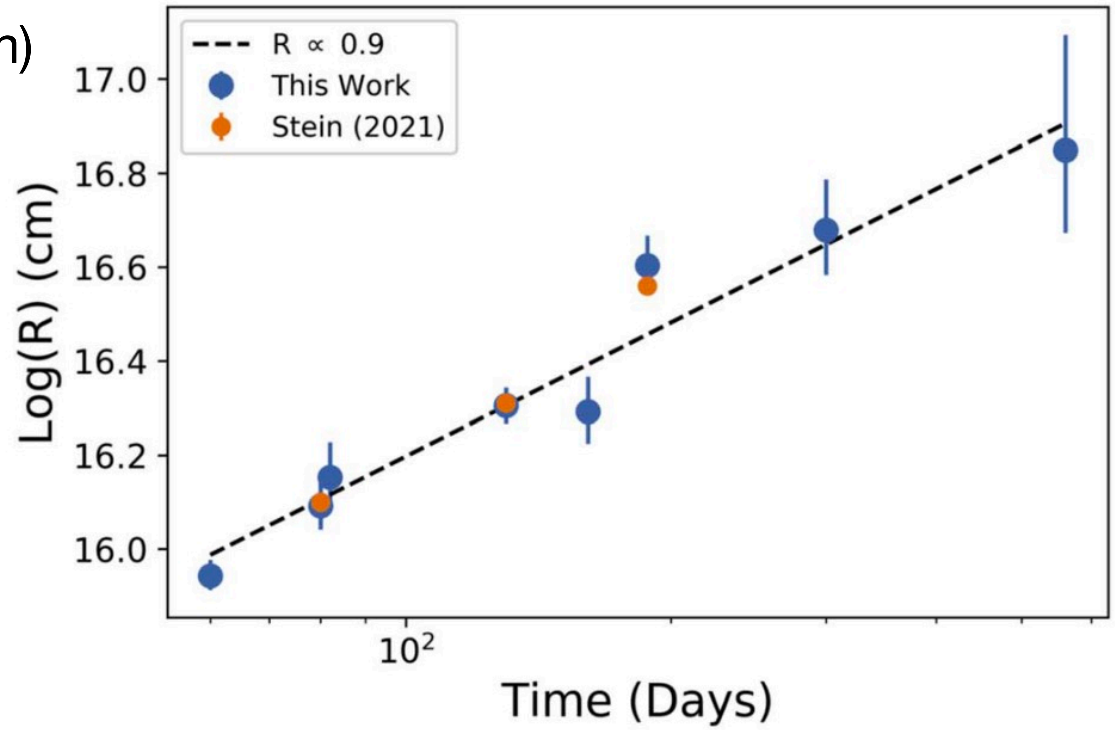

Different from a free-expansion solution: $R \propto t$ and the Sedov solution: $R \propto t^{2/5}$

What physics determines the dynamics of $R(t)$ in radio TDEs?

Evolution of radio-emitting region in AT2019dsg

Matsumoto et al. (2021)

SSA model + equipartition analysis

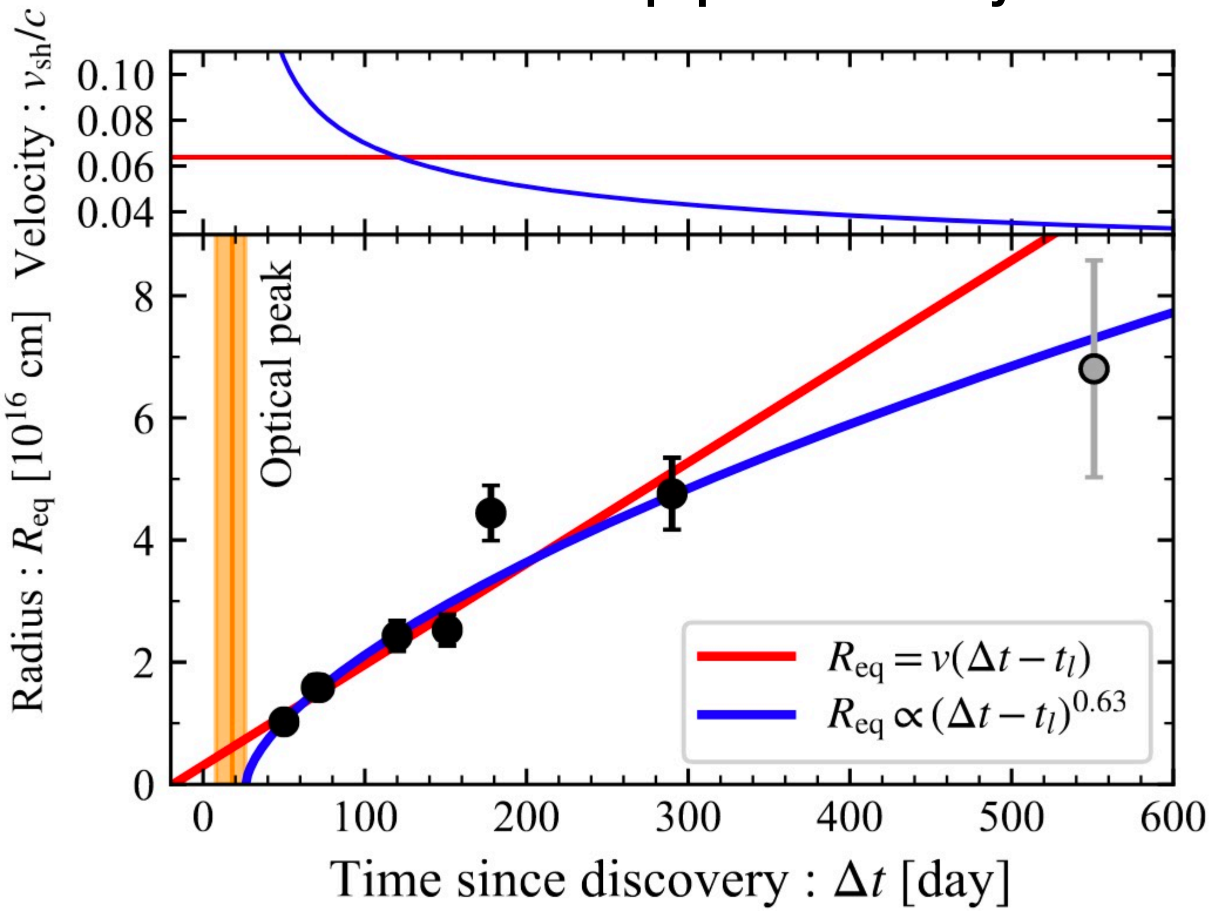

Our model Hayasaki & Yamazaki (2023)

1. A time-dependent, non-relativistic, one-dimensional spherically symmetric shell model as a radio emitter
   Chevalier A. R (1982); Longair S. M (2011)
2. Electrons in the shell are accelerated to relativistic energies with $\propto \gamma^{-p}$, producing synchrotron emissions e.g., Chevalier A. R (1998)
3. Not simple point source explosion but continuous mass injection at a rate proportional to $\dot{M}_{\rm fb}$ from the disk. This is unique to TDEs
4. Strong gravity unlike SNRs or PWNs

Schematic diagram of spherically-symmetric radio-emitting shell

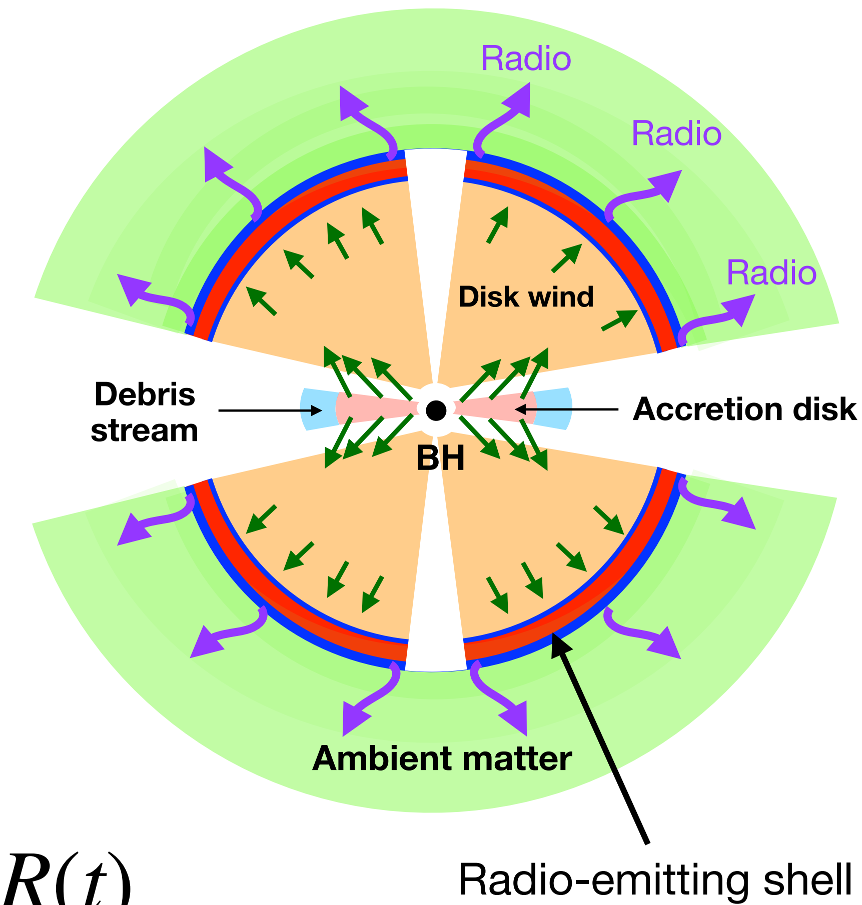

In this work, we focus on dynamics of $R(t)$

Model details

Assumptions

1. Spherically symmetric shell
2. Thin shell approximation: $\Delta R \ll R$
3. The thin shell is formed at $r = r_0$ and $t = t_0$
4. Initial velocity: $\dot{R}(t = t_0) = v_0$, where $v_0 \sim 0.1c$
5. For simplicity, thermal pressure and the gravitational force are neglected

Schematic view of our model

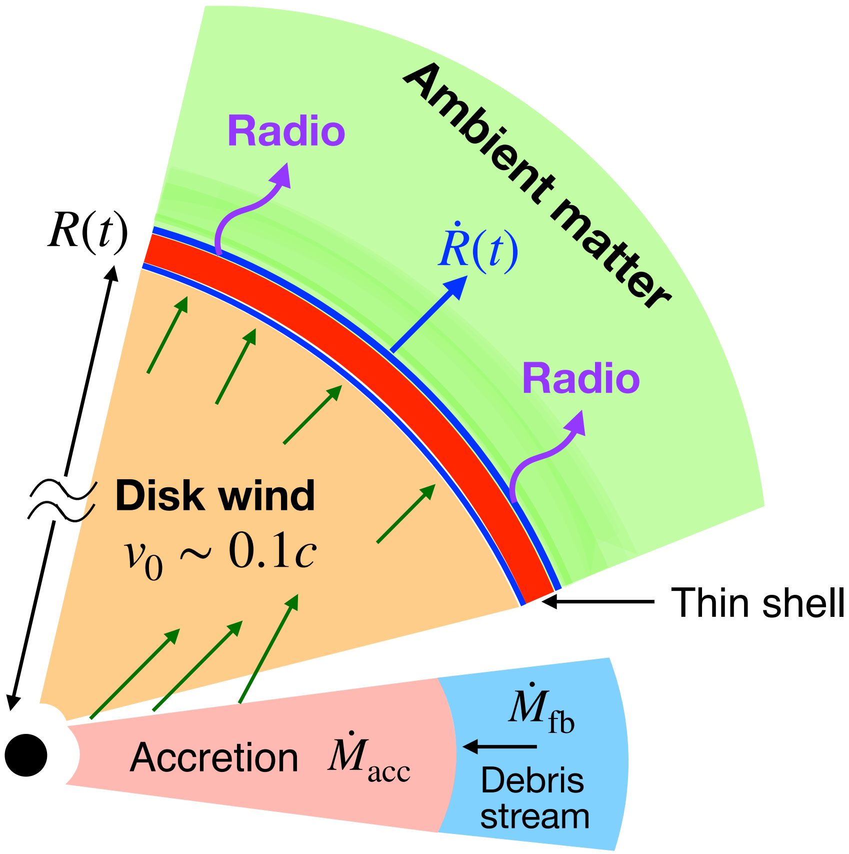

In this work, we focus on the dynamics of $R(t)$

Equation of motion of the shell

- Momentum conservation law between t and $t + \Delta t$

$$\boxed{F_{\rm ej}\Delta t} = M(t + \Delta t)\dot{R}(t + \Delta t) - M(t)\dot{R}(t)$$

Impulse

at $\Delta t \to 0$ limit

- Equation of motion of the thin shell

$$M\frac{d^2R}{dt^2} = \left[1 - \epsilon\left(\frac{\dot{R}}{V_0}\right)\right] F_{\rm ej} - F_{\rm am}$$

- Shell mass:

$$M = M_{\rm ej} + M_{\rm am} + \Delta m$$

- Ram pressure force due to disk wind:

$$F_{\rm ej} = 4\pi R^2(\rho_{\rm ej}\dot{R}^2)$$

- Ram pressure force due to ambient matter:

$$F_{\rm am} = 4\pi R^2(\rho_{\rm am}\dot{R}^2)$$

Dimensionless equation of motion

$$\ddot{y} = \left[(n-1)\left[x+\epsilon(1-y)\right]^{-n}\left[2\dot{y}-\epsilon\dot{y}^2-\frac{1}{\epsilon}\right]+\eta\epsilon(n-1)y^{2-s}\dot{y}^2\right]$$
$$\Big/\left[\left[x+\epsilon(1-y)\right]^{1-n}-\frac{\eta\epsilon(n-1)}{3-s}(y^{3-s}-1)-\delta\epsilon(n-1)-1\right]$$

$$x \equiv \frac{t}{t_0},$$
$$y \equiv \frac{R(t)}{r_0},$$
$$\dot{y} \equiv \frac{dy}{dx} = \frac{\dot{R}(t)}{V_0},$$
$$\ddot{y} \equiv \frac{d^2y}{dx^2} = \ddot{R}(t)\frac{t_0}{V_0}$$

Five different dimensionless parameters: $(n, s, \epsilon, \eta, \delta)$

$$n = -\frac{\ln(\dot{M}_{\rm ej}/\dot{M}_0)}{\ln(t/t_0)} \quad s = -\frac{\ln(\rho_{\rm am}/\rho_{\rm am,0})}{\ln(r/r_0)} \quad \epsilon = \frac{V_0}{v_0} \quad \eta = \frac{\rho_{\rm am,0}}{\rho_{\rm ej,0}} \quad \delta = \frac{\Delta m}{(4\pi\rho_{\rm ej,0}r_0^3)}$$

$(V_0 = r_0/t_0)$

We solve the dimensionless equation of motion numerically using the RK method

Analytical solutions

1. Approximate solution around $t = t_0$ (near the time origin)

$$y(x) = y(x_0) + \dot{y}(x_0)(x - x_0) + \frac{1}{2}\ddot{y}(x_0)(x - x_0)^2 + \frac{1}{6}\dddot{y}(x_0)(x - x_0)^3 + \mathcal{O}\left((x - x_0)^4\right)$$

$$\approx 1 + \frac{1}{\epsilon}(x - x_0) - \frac{1}{2}\frac{\eta}{\epsilon^2\delta}(x - x_0)^2 + \frac{1}{6}\frac{\eta}{\epsilon^3\delta}\left(3\frac{\eta}{\delta} + s - 2\right)(x - x_0)^3$$

2. Asymptotic solution at $R \gg r_0$

$$M\frac{d^2R}{dt^2} = \left[1 - \epsilon\left(\frac{\dot{R}}{V_0}\right)\right]F_{\rm ej} - F_{\rm am} \longrightarrow M_{\rm am}\frac{d^2R}{dt^2} = -F_{\rm am}$$

$$s = -\frac{\ln(\rho_{\rm am}/\rho_{\rm am,0})}{\ln(r/r_0)}$$

$$\longrightarrow R(t)\ddot{R}(t) = (s-3)\dot{R}(t)^2 \longrightarrow R(t) \propto t^{1/(4-s)}$$

Momentum-driven snow plow phase

Comparison between numerical and approximate solutions near the origin

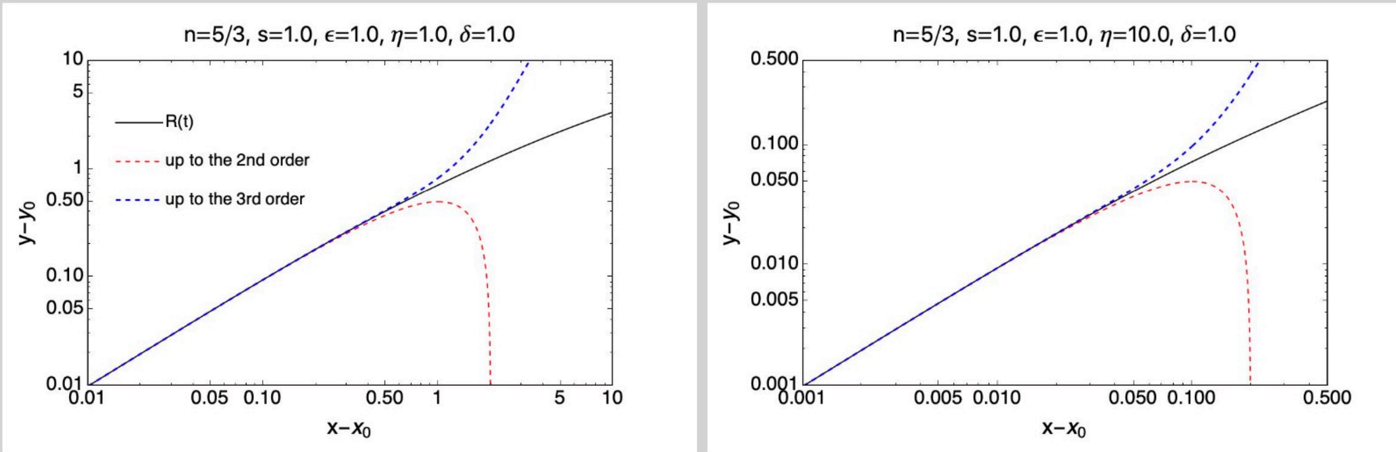

(a) $(y = R(t)/r_0, x = t/t_0)$ (b)

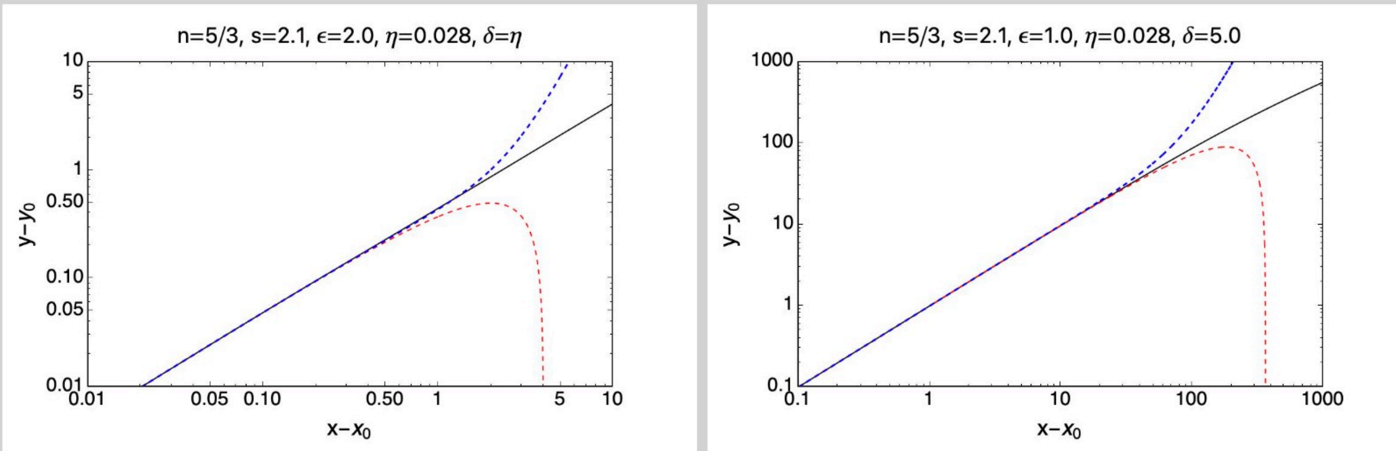

(c) (d)

The numerical solutions agree with the approximate solutions for various parameters

Comparison between numerical and asymptotic solutions

Power-law time
index for shell radius

$$m \equiv \frac{d \ln(y - y_0)}{d \ln(x - x_0)}$$

$$y = R(t)/r_0, x = t/t_0$$

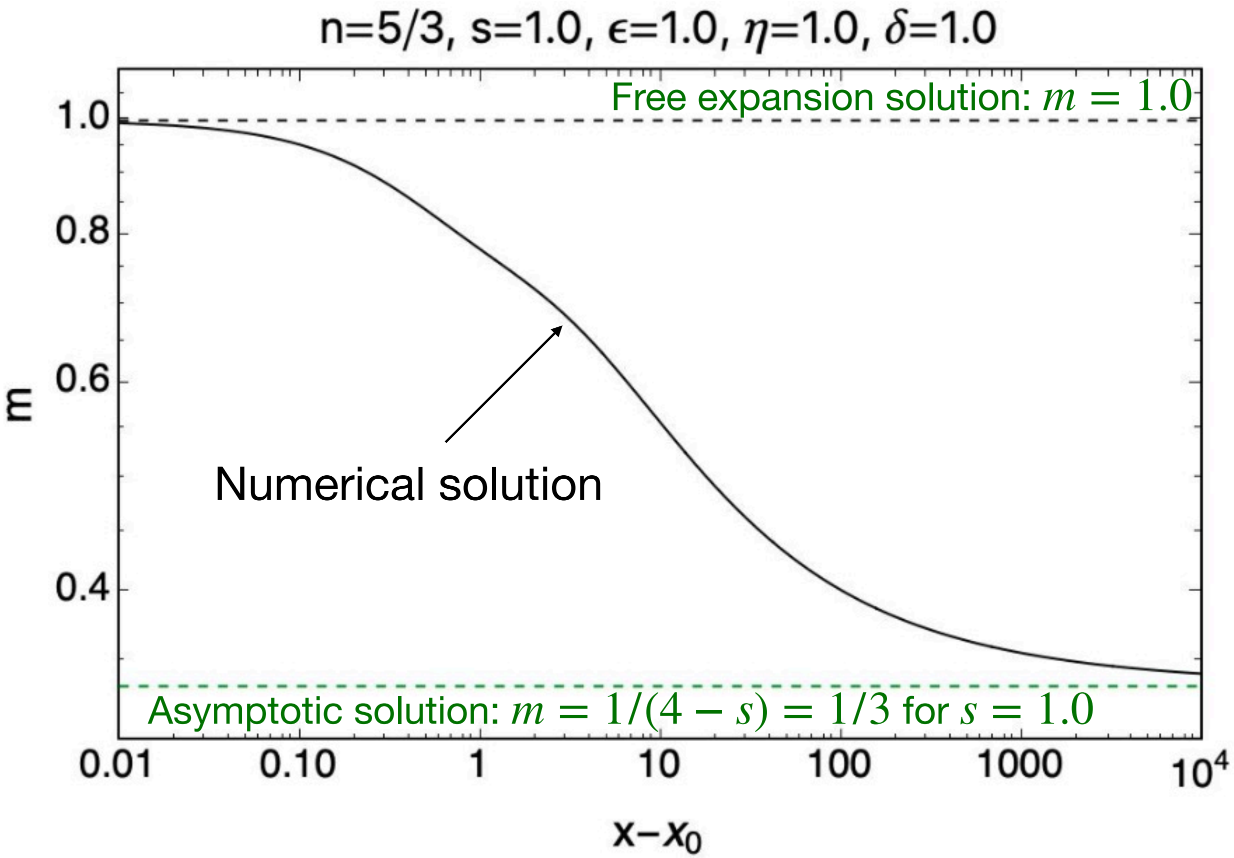

1. A slightly limp curve of the numerical solution is due to $F_{\rm ej}$
2. Numerical solution asymptotes the power law of time with 1/(4-s)

Application to a radio-emitting TDE: AT2019dsg

$$r_0 = r_\mathrm{t} = \left(\frac{M}{m_*}\right)^{1/3} r_* \sim 1.1 \times 10^{13}\,\mathrm{cm} \left(\frac{M}{10^{6.7}\,M_\odot}\right)^{1/3} \left(\frac{m_*}{M_\odot}\right)^{-1/3} \left(\frac{r_*}{R_\odot}\right),$$

$$t_0 = \sqrt{\frac{r_*^3}{Gm_*}} \sim 1.6 \times 10^3\,\mathrm{s} \left(\frac{m_*}{M_\odot}\right)^{-1/2} \left(\frac{r_*}{R_\odot}\right)^{3/2},$$

$$\frac{V_0}{c} = \sqrt{\frac{GM}{c^2 r_\mathrm{t}}} = \left(\frac{M}{m_*}\right)^{1/3} \left(\frac{Gm_*}{r_*}\right)^{1/2} \sim 0.25 \left(\frac{M}{10^{6.7}\,M_\odot}\right)^{1/3} \left(\frac{m_*}{M_\odot}\right)^{1/6} \left(\frac{r_*}{R_\odot}\right)^{-1/2},$$

$$M_0 = \dot{M}_0 t_0 = \frac{f}{3} m_* \left(\frac{t_0}{t_\mathrm{mtb}}\right) \simeq 6.7 \times 10^{-6}\,M_\odot \left(\frac{f}{0.1}\right) \left(\frac{M}{10^{6.7}\,M_\odot}\right)^{-1/2} \left(\frac{m_*}{M_\odot}\right)^{3/2},$$

$$t_\mathrm{mtb} = \frac{\pi}{\sqrt{2}} \left(\frac{M}{m_*}\right)^{1/2} t_0 \sim 92\,\mathrm{day} \left(\frac{M}{10^{6.7}\,M_\odot}\right)^{1/2} \left(\frac{m_*}{M_\odot}\right)^{-1} \left(\frac{r_*}{R_\odot}\right)^{3/2}$$

$$\rho_\mathrm{ej,0} = \frac{\dot{M}_0}{4\pi r_0^2 v_0} \sim 1.3 \times 10^{-12}\,\mathrm{g/cm^3} \left(\frac{f}{0.1}\right) \left(\frac{\epsilon}{1.0}\right) \left(\frac{M}{10^{6.7}\,M_\odot}\right)^{-3/2} \left(\frac{m_*}{M_\odot}\right)^{5/2} \left(\frac{r_*}{R_\odot}\right)^{-3}$$

$$\rho_\mathrm{am,0} = \rho_\mathrm{obs} \left(\frac{r}{r_0}\right)^{s} \sim 1.7 \times 10^{-14}\,\mathrm{g/cm^3} \left(\frac{n_\mathrm{ext}}{10^{3.56}\,\mathrm{cm^{-3}}}\right) \left(\frac{r}{10^{16.15}\,\mathrm{cm}}\right)^{2.1} \left(\frac{r_0}{r_\mathrm{t}}\right)^{-2.1}$$

$$\eta\,\epsilon = \frac{4\pi r_0^3 \rho_\mathrm{obs}}{\dot{M}_0\,t_0} \left(\frac{r}{r_0}\right)^{s} \sim 2.8 \times 10^{-2} \left(\frac{f}{0.1}\right)^{-1} \left(\frac{n_\mathrm{ext}}{10^{3.56}\,\mathrm{cm^{-3}}}\right) \left(\frac{r}{10^{16.15}\,\mathrm{cm}}\right)^{2.1} \left(\frac{r_0}{r_\mathrm{t}}\right)^{0.9} \left(\frac{M}{10^{6.7}\,M_\odot}\right)^{1/2} \left(\frac{m_*}{M_\odot}\right)^{-3/2}$$

$$\Delta m = \delta\epsilon \dot{M}_0 t_0 \simeq 6.7 \times 10^{-6}\,M_\odot \left(\frac{f}{0.1}\right) \left(\frac{\delta}{1.0}\right) \left(\frac{\epsilon}{1.0}\right) \left(\frac{M}{10^{6.7}\,M_\odot}\right)^{-1/2} \left(\frac{m_*}{M_\odot}\right)^{3/2}$$

Six normalization parameters and five dimensionless parameters should be decided for the comparison purpose

Comparison with the observation

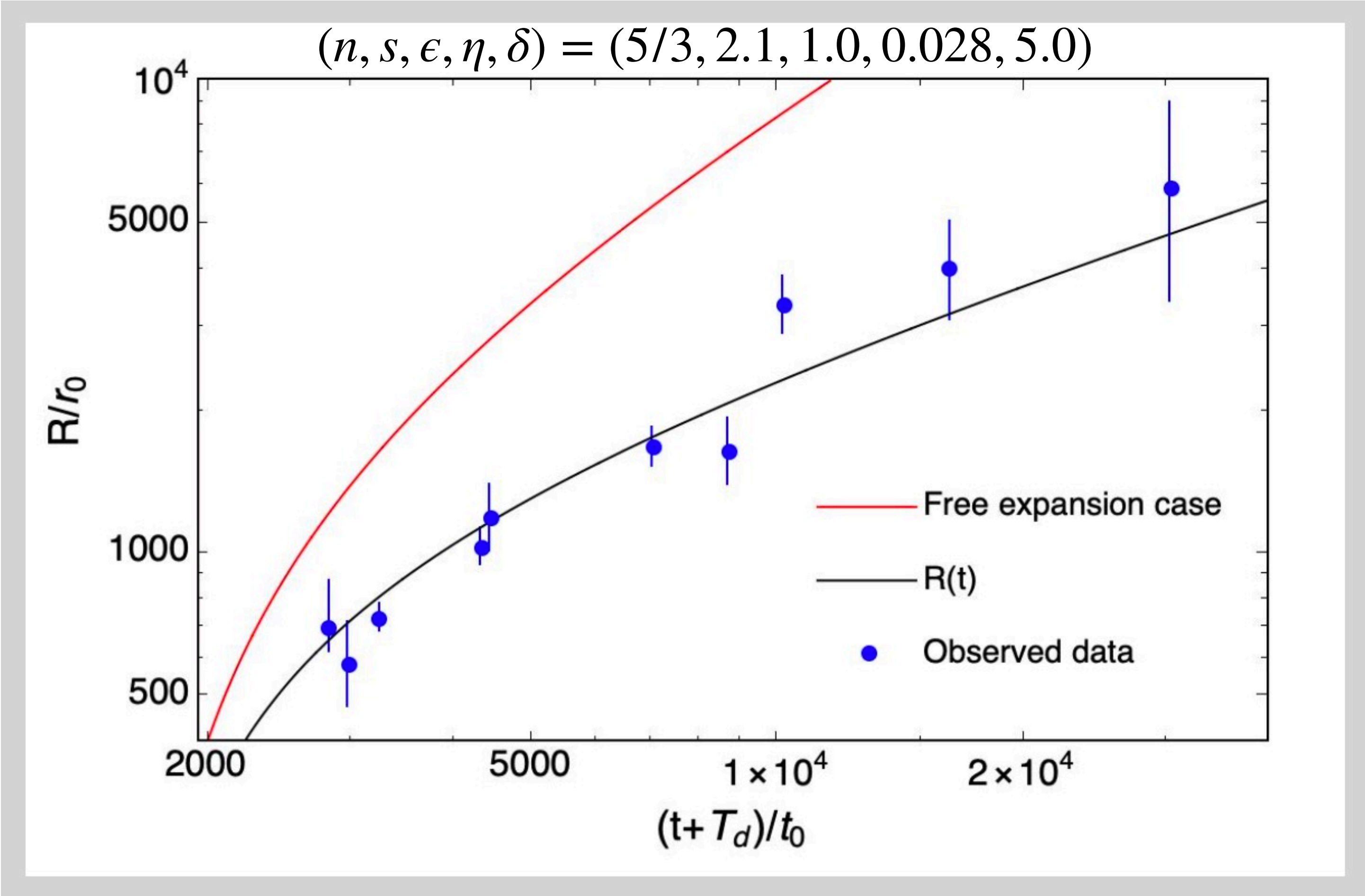

$T_{\rm d} \sim 40\,{\rm days}$: onset of OUV emissions

Our model can explain the evolution of the observed radio-emitted region

Summary

We have constructed a time-dependent, one-dimensional spherically symmetric, geometrically thin shell model to explain the evolution of radio-emitting region in TDEs. Our conclusions are summarized below:

1. The numerical solutions agree with two types of analytical solutions that we derived
2. Our model explains well the observed radio emission size evolution in AT2019dsg

Discussion

1. Five main parameters for our models: $(n, s, \epsilon, \eta, \delta)$ are limited to some extent by observation and theory. Determining the optimal set is a future task.
2. Thermal pressure and SMBH gravity should be included (Hayasaki & Yamazaki. in prep)
3. Synchrotron spectra will be calculated with $R(t)$, allowing a direct comparison between shell dynamics and observations.
4. Application to the other radio detected TDEs (ASASSN-14li, etc)
5. Initial shell formation and multi-dimensional effects on it (Hu, Price,…& Hayasaki et al. 2024, in prep)

Thank you for your attention